Non-intrusive partial discharges investigations on aeronautic motors

Thibaut Billard, Cédric Abadie, Bouazza Taghia

Non-Intrusive Partial Discharges Investigations on Aeronautic Motors

Thibaut Billard, Cedric Abadie, and Bouazza Taghia
IRT Saint-Exupery

CITATION: Billard, T., Abadie, C., and Taghia, B., "Non-Intrusive Partial Discharges Investigations on Aeronautic Motors," SAE Technical Paper 2016-01-2058, 2016, doi:10.4271/2016-01-2058.

Abstract

The present paper reports non-electrically intrusive partial discharge investigations on an aeronautic motor. Relevancy, robustness and repeatability of partial discharge testing procedures, both on insulating materials characterization and on operating aeronautic equipment are essential to ensure reliability of the aircraft systems. The aim of this paper is to be the very first step of defining such procedures and the associated test equipment.

To do so, the paper will start by providing an understanding of partial discharge phenomena and will review typical more electrical aircraft architecture. Key characteristics causing partial discharge risk to increase will be highlighted. The impact of harness length, high performance power electronics and voltage level increase on insulation system is demonstrated.

Then, an analysis is carried out from motor design perspective to find out which test procedure is relevant to assess each insulation system performance both at atmospheric and reduced pressures. The study helps to realize the benefits of using multiple test sample and procedure to assess insulation system performance level through the design process of the motor. It is shown that a good agreement observed between stator and representative samples.

This paper will also review the ability of the non-intrusive test method to detect partial discharge with a full scope of voltage signal from AC to impulse voltage and under different pressures. The paper concludes with an analysis of results and thoughts about future work regarding motor design taking into account partial discharge risk and evolution of proposed procedure.

Introduction

Background

Optimization of energy sources aboard aircraft and permanent improvements in more electric technologies are pushing the aeronautic industry to aim for the more electrical aircraft (MEA).

Indeed, electric energy offers numerous benefits in aircrafts. First, power generation, distribution and conversion are easier because being more accurate and flexible than pneumatic or hydraulic energy control. Then, significant mass reduction seems more likely to be achieved than with traditional hydraulic systems needing large, heavy and maintenance intensive distribution system.

But, this shift towards MEA is not without consequences on the electrical stress the insulation system has to withstand. Thus, with primary voltage increasing, power distribution architecture evolution and high power density power electronics, partial discharge is now a serious cause of concern for aircraft integrator, system designer and component manufacturer. Once partial discharges are occurring regularly, degradation of the insulation system until premature failure of the aircraft system is irremediable.

Scope and goal of the work

This topic of interest has already been discussed by several key actors of the aerospace industry, research center such as US Air force laboratory or international academic actors. All acknowledge that partial discharge risk in a harsh aeronautic environment where pressure, temperature and humidity variation, electrical stress created by inverter and harness length and weight increase. [1, 2, 3, 4]

Among key issues of aeronautic companies that has to be dealt with at IRT Saint-Exupéry, two will be addressed in this paper and will be the main contribution.

First, the ability to accurately detect partial discharge, from material characterization tests to full system analysis during operation, in an electrically non-intrusive way and under representative aeronautic environment. Secondly, determine and specify a relevant set of test procedure and characterization equipment to make informed decision during the design of electric component to take into account partial discharge risks prior to qualification tests and prototype manufacturing. In order to illustrate the full scope of the analysis, a typical 540VDC aeronautic stator has been designed.

Outline

First, partial discharge key points and its consequences on insulation system will be highlighted. In a second step, key features of more electrical aircraft will be recalled, especially those in relationship to the reliability of the insulation system.

Then, details of the stator will be presented along with the typical insulation system used. An analysis will be made on the creation of electrical stress on the insulation system of the stator. Before providing test results and analysis, test procedure logic will be underlined as first step towards a robust characterization procedure. Finally, some discussions regarding results, modification of test procedure and future work will be presented.

Partial Discharge Basics

What is a Partial Discharge? IEEE Definition

According to IEEE standard definition [5] a partial discharge (PD) is:

An electrical discharge that only partially bridges the insulation between conductors. A transient gaseous ionization occurs in an insulation system when the electric stress exceeds a critical value, and this ionization produces partial discharges.

Paschen's Law

One well known threshold for partial discharge inception is the so-called Paschen minimum at 320-330V peak in air at room temperature and standard humidity between parallel metallic electrodes. The so-called Paschen curve, plotted either experimentally or analytically after Townsend theory, represents the partial discharge inception voltage (self-sustained discharge) in aforementioned conditions. Under this curve, no self-sustained partial discharge could happen (figure 1).

Consequences of Partial Discharge

Partial discharge events have been known and studied for more than a century, starting with Paschen, Peek and Townsend among others. Partial discharges are feared because they contribute to the degradation of the insulation system and lead to its premature failure [6]

- Chemical effect (ozone creation, nitric acid in the presence of moisture).
- Thermal effect (hot needle on the insulation system)
- Mechanical effect (ion and electron erosion, destruction of polymeric chemical bond)
- UV creation

Partial Discharge in More Electrical Aircraft

In relation with aircraft network voltage, the Paschen minimum is 230V AC RMS. It means that, for conventional aircraft electric system using 28V DC and 115 VAC RMS, partial discharge risk was non-existent.

But, with the recent increase in voltage from 115 V AC to 230 V AC or ±270 VDC on HVDC network, that risk has to be taken into account in designing equipment and in qualification process. As shown on figure 1, at 540V peak, partial discharge could occur in air at atmospheric pressure between parallel metallic electrodes at a distance of 40µm or less. At 100mbars, partial discharge could occur up to a distance of 0.35mm. Partial discharge risk is thus highly linked to pressure level.

Obviously, air is not the only insulation system in aircraft equipment and geometry is highly non-uniform so direct calculation are hazardous. Still, there could be a combination of pressure, distance, voltage and electric field unfavorable enough to reach partial discharge inception voltage in air between insulation or in a void within the insulation system if the applied voltage is above Paschen minimum.

Partial Discharge Inception and Extinction Voltage

According to IEEE Standard [5], partial discharge inception voltage (PDIV) is

The lowest voltage at which continuous partial discharges (PDs) above some stated magnitude (which may define the limit of permissible background noise) occur as the applied voltage is increased. Many factors may influence the value of PDIV, including the rate at which the voltage is increased as well as the previous history of the voltage applied to the winding or component thereof

And partial discharge extinction voltage (PDEV) is:

The highest voltage at which partial discharges (PDs) above some stated magnitude (which may define the limit of permissible background noise) no longer occur as the applied voltage is gradually decreased from above the inception voltage. Many factors may influence the value of PDEV including the rate at which the voltage is decreased as well as the previous history of the voltage applied to the winding or component thereof. In most cases, PDEV is less than PDIV.

PDIV and PDEV could be expressed either at RMS or peak voltage depending on the applied voltage during test.

During partial discharge test of equipment, PDIV and PDEV are usually a representation of the insulation system quality. In other words, it represents its ability to withstand a defined voltage level before partial discharge occurs.

It is thus of a critical importance to that tests are robust, easy to reproduce and relevant for the foreseen application. It is also important to have an accurate PDIV and PDEV measurement methods that could be applied indistinctly on all the aforementioned configuration. From simple material characterization test at atmospheric pressure, to an operating system in a low pressure environment.

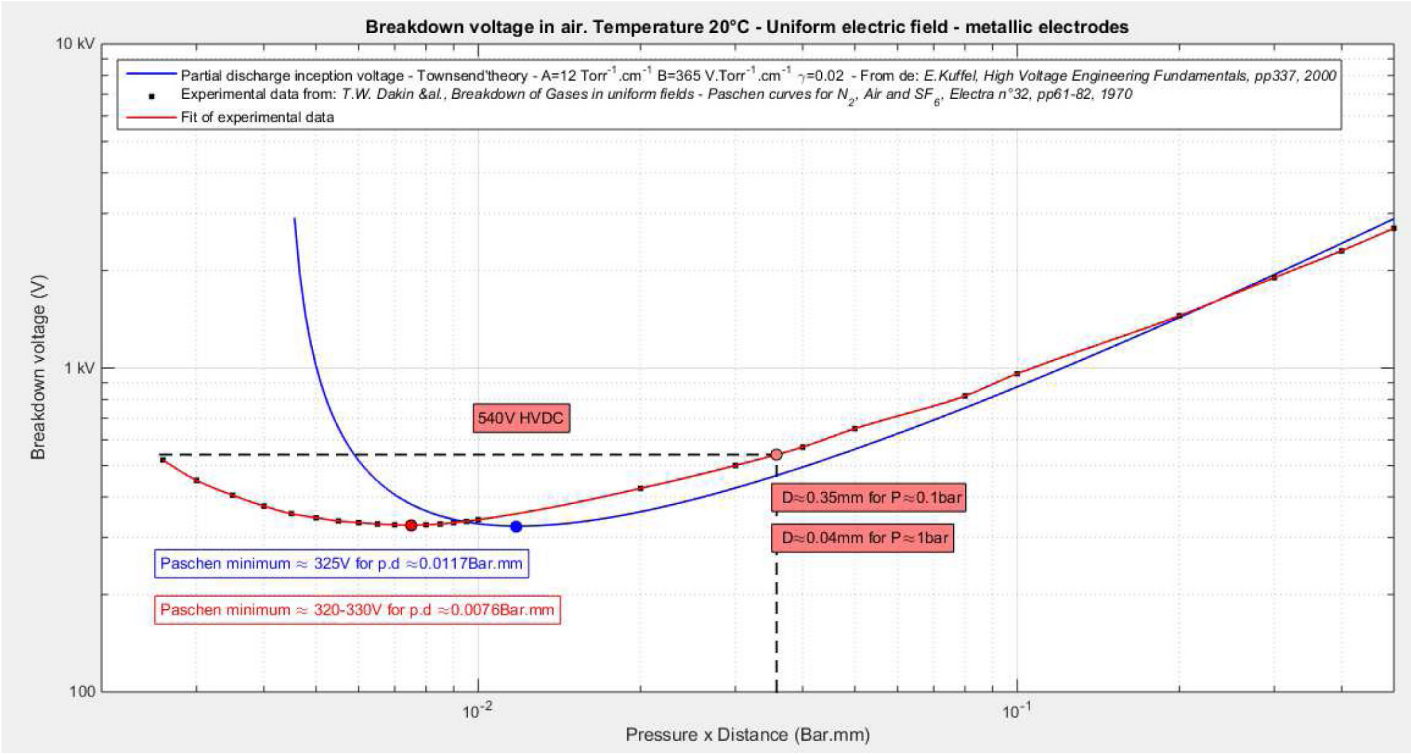

Figure 1. Paschen curve for air at room temperature conditions between parallel metallic electrodes.

Failure of reporting an equipment subject to partial discharge could have dramatic consequence on its reliability, leading to short-circuits creating electrical arcs. Safe level of target PDIV and PDEV should be set in order to ensure equipment are PD free during operational life of the system.

More Electrical Aircraft Paradigm

The MEA approach underlines the use of electrical system for non-propulsive application such as environmental control systems (ECS), electric driven hydraulic pump or flight control actuation. Other applications such as electrical taxiing or anti-icing are also considered for electrification. In other words, a more electrical aircraft has no on-engine hydraulic power generation and bleed air off-takes but more and more power electronics and electric motors.

Current More Electrical Aircrafts

Current commercial aircrafts such as A380, B787 and A350, military aircraft such as F-35 fighter or unmanned air vehicles (UAV) are already displaying a number a MEA technologies. This paragraph details such technologies in order to better understand partial discharge risk in the more electrical aircraft.

B787 Electrical Overview

Boeing 787 is a large step forward in the more electrical aircraft. Bleed air is no longer taken from the engines and the majority of power used in actuators comes from electricity. A key feature is the adoption of 230 V AC electric power compared with the conventional 115 V AC generation.

Each of the two jet engine supplies two starter/generator of 250 kVA 230V AC VFG resulting in a total generated power of 500 kVA per channel. Two 225 kVA APU starter/generator are also supplying 230 V AC to the electric power distribution system. The electric power distribution system is directly powering some load with 230 V AC but is also converting into 115 V AC and 28 V DC to feed conventional systems.

The bleed-less air system is of particular interest since it means that air for ECS and pressurization systems needs to be pressurized electrically with four large compressors drawing around a total of 500 kVA. Wing anti-icing is also provided by electrical heating mats requiring around 100kVA of electrical power. The replacement of engine driven pumps (EDP) by electrically driven pumps means an additional 400kVA is needed.

A350 Electrical Overview

The A350 electrical system could be seen as an evolution of the A380 one, with the same “two hydraulic and two electric” networks logic. Aside with numerous electric actuators like Electro-mechanical Actuator (EMA), Electro-Hydrostatic Actuators (EHA) and Electrical Back-Up Actuator (EBHA) as in the A380, the main change is the increase of primary voltage from 115V AC to 230 V AC with four VFG, each one supplying 100kVA of electric power and one variable speed APU supplying 150 kVA. Since ground power connection is 115 V AC, a reversible autotransformer unit (ATU) is used as a conversion to electrically start the engines and to convert 230 V AC into 115 V AC.

Key Role of Highly Integrated Power Electronics

A key enabler of such development is the breakthrough in high power density, high voltage and reliable silicon-based power semiconductor switching device such as insulated gate bipolar transistor (IGBT).

It is expected that state-of-the-art switching device such as Silicon Carbide (SiC) or Gallium Nitride (GaN) will dramatically improve inverter drive, converters, motor controller and other semiconductor based power systems power density, fulfilling at the same time mass reduction objective and electric power increase. Since a significant part of power electronics system mass is thermal management system including active liquid cooled loop, innovation in thermal management will even more increase power density while simplifying maintenance operations.

It will be shown later in this article how the evolution of power electronics towards fast switching in the more electrical aircraft with HV AC and HV DC network increased primary voltage is putting even more stress on motor insulation system. [7, 8, 9, 10].

Electromechanical Chain

An MEA electromechanical chain is supplied by the electric power network. It could be an HVDC network or a variable frequency 230 V AC network for power hungry systems such as ECS. Then a power electronic module is used to adapt the power supply to the motor (or actuator) needs. An input filter could be placed network side to avoid altering network stability. An EMC filter module could be placed motor side to limit conducted emission through a non-shielded harness.

Power transmission is then made by a harness which could have different length depending on the motor location compared to the power electronics module. This power transmission line size and type depends on the number of signals to transmit and its current/voltage rating.

Finally, the energy conversion from electric energy into magnetic then mechanical energy is realized by the motor. Usually, permanent magnet synchronous motor are used because of their high power density. It is often assumed that the motor is the weakest link of the electromechanical chain regarding partial discharge risk.

Combined Effect of Harness Length and Rise Time on Motor Terminals Overvoltage

One of the main problem when connecting an inverter drive to an electric machine is the presence of overvoltage at the motor terminals. To better understand this mechanism, one should focus on one voltage pulse coming from the inverter drive at a time. A reflection phenomenon is occurring on an incident wave travelling at a fraction of the speed of light in a cable (depending on the physical construction of the cable) when there is an impedance mismatch between the cable, acting as a transmission line, and the impedance at the end of the cable. At the cable's end (or at motor terminals), the reflected wave is added to the incident wave and the total voltage is thus increased. In other words, when pulse like voltage signal is transmitted along a line, which is not terminated by its characteristics impedance, reflections could occur. [11]

Reflexion coefficients are function of the impedance Z of each component at the input and output of the transmission line

$$\Gamma_{mot} = \frac{Z_{motor} - Z_{harness}}{Z_{motor} + Z_{harness}} \tag{1}$$

$$\Gamma_{inv} = \frac{Z_{inverter} - Z_{harness}}{Z_{inverter} + Z_{harness}} \tag{2}$$

From a practical point of view, the impedance of an electric motor is always larger than the cable impedance. The inverter drive is usually of low impedance, so when the reflected wave reaches the inverter, a new reflexion (negative) occurs. In fact, the maximum voltage at motor terminals (including reflexion amplitude), deriving from the transmission line theory, could approximately double in case of large impedance mismatches. The total amplitude is also function of the rise time relative to the travelling speed and of the cable length. Larger overvoltage could nonetheless occurs in specific conditions with bipolar pulse of a very short time.

Simple lossless transmission line calculation based on delay allows the evaluation of the maximum overvoltage at motor terminals after a length L of harness at any time t knowing both reflexion coefficients, the travelling time T and the input voltage at the beginning of the line V(t).

$$V(L,t) = (1 + \Gamma_{mot}) \cdot \sum_{i=0}^{n} {\Gamma_{mot}}^{i} \cdot {\Gamma^{i}}_{inv} \cdot V(t - (2i+1)T) \tag{3}$$

Further simplifications are possible if the shape of the input voltage V(t) if defined. For example, a simple ramp from zero to E voltage with a rise time parameter t_r.

$$If\ t < 0\ then\ V(t) = 0$$
$$If\ t \geq 0\ and\ \ t < t_r\ then\ V(t) = E \cdot \left(\frac{t}{t_r}\right)$$
$$If\ t \geq t_r\ then\ V(t) = E \tag{4}$$

It can be shown that the maximum voltage will be reached at t=t+ t_r. From equation 3, introducing above simplifications the maximum voltage at motor terminals is.

$$V(L, T + t_r) = \frac{Z_{harness}}{Z_{harness} + Z_{inverter}} (1 + \Gamma_{mot}) \cdot \left[1 + \Gamma_{mot}\Gamma_{inv} \cdot \left(\frac{t_r - 2 \cdot T}{t_r}\right)\right] \tag{5}$$

An overvoltage chart could be calculated using the following extreme assumptions to have a clear qualitative understanding of the interaction between travelling time, rise time of input voltage and overvoltage coefficient defined as the ratio of maximum motor terminal voltage on input voltage.

- Harness impedance: 75Ω
- Motor impedance : 1GΩ
- Inverter impedance : 1nΩ

It is clear from figure 2 that the shorter the rise time, the shorter the harness critical length for a maximum overvoltage. For standard aeronautic harness, a few dozen of ns delay is equivalent to a few meter length cable. This figure is very similar to the one found in EIC 60034-18-41 standard [12].

When using motor impedance as a parameter, it is demonstrated in figure 3.a that the maximum overvoltage is decreasing as the motor impedance is lower. Figure 3.b is provided to give more details regarding successive reflexion phenomena.This is expected since the motor reflexion coefficient is lower.

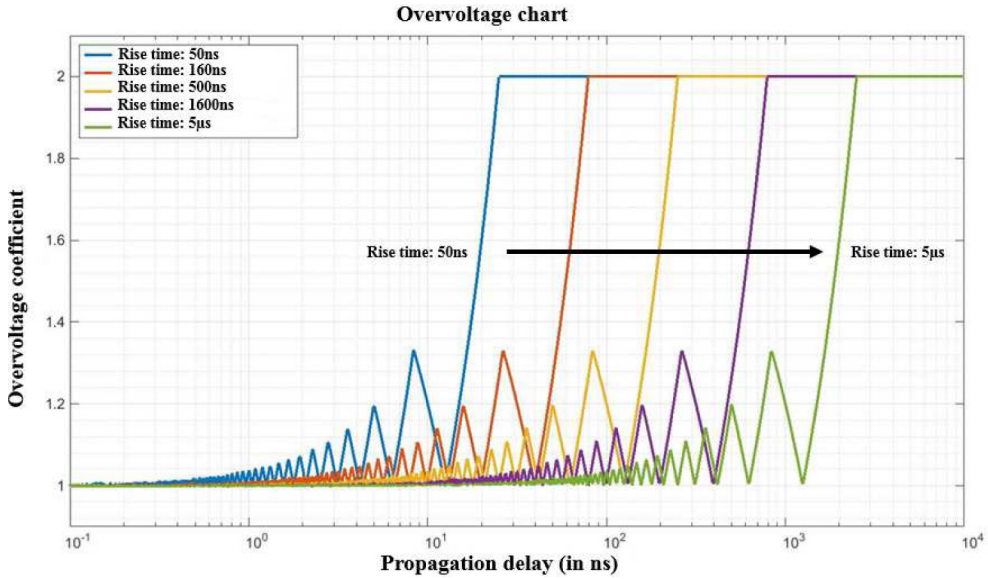

Figure 2. Overvoltage chart showing maximum voltage at motor terminal function of input voltage travelling time and rise time.

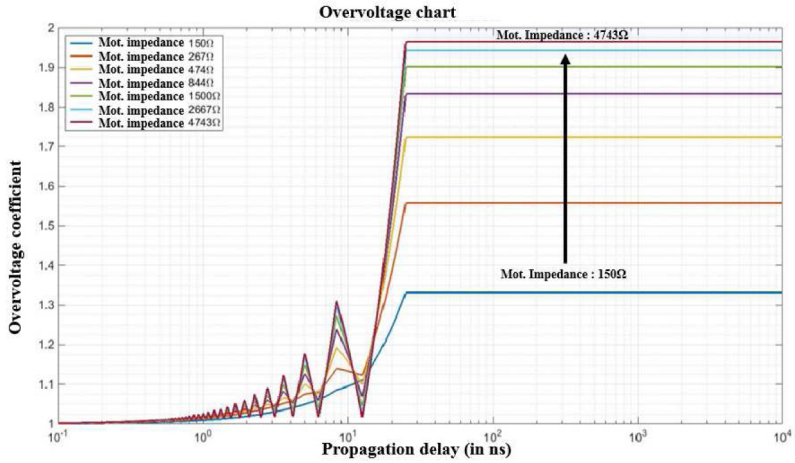

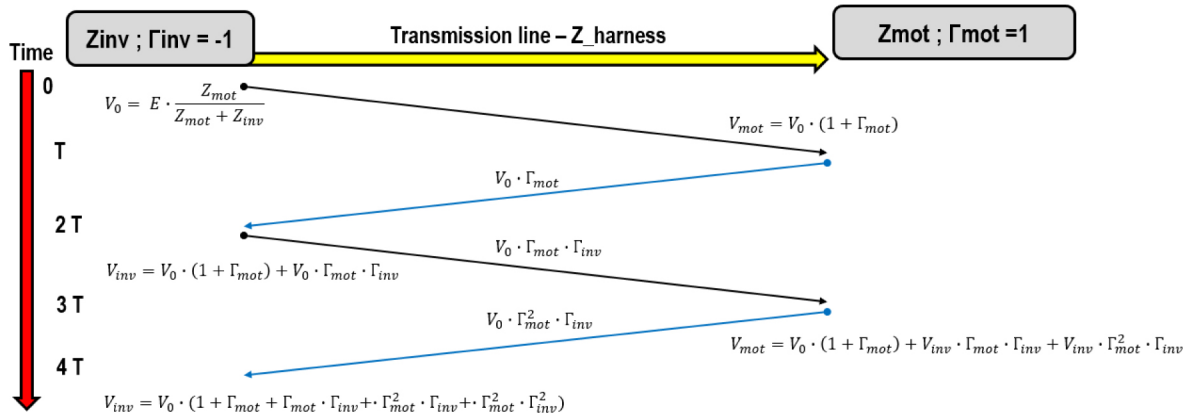

Figure 3. a (top). Overvoltage chart showing maximum voltage at motor terminal function of input voltage travelling time and motor impedance for a rise of 50ns and inverter impedance of 100mΩ. b (bottom) Transmission line diagramm

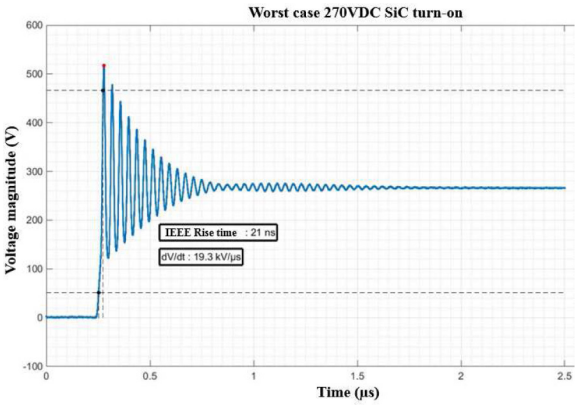

Figure 3.c. Worst case SiC turn-on voltage with modified grid voltage and low current from IRT power electronics measurements

Indeed, in figure 3.c, a worst case turn-on switching of a SiC with a 270 V DC bus is plotted after measurement at the output of the inverter drive. By voluntary tweaking the grid voltage and current, the parasite capacitance of the switch could create large overvoltage at the entrance of the transmission line even before harness reflexion phenomena occurs. In such conditions, very large overvoltage could be expected at motor terminals and either operational measurements, safety coefficient or overvoltage simulation should be carried out to interpret partial discharge voltage results from “off-line” testing.

Impulse Voltage Propagation Through Windings

Most studies focus on voltage at motor terminals caused by impedance mismatch and rise time. But another important aspect of the way the electrical insulation is affected by a PWM inverter drive, is the shape of the turn-to-turn stress. Indeed, some failures are caused by the voltage distribution in the winding. While voltage distribution along a winding is usually uniform at all time under 50Hz voltage supply, (the winding is seen as a simple inductance bridge),voltage distribution is very non-uniform under PWM voltage because of the propagation time of the pulse in the winding.

Indeed, the voltage is not propagating immediately along the winding causing a delay between turns. High frequencies dielectrics losses in the insulation system and iron losses in the stator frame are decreasing rise time and smoothing the eventual overvoltage alongside the coil. At the same time, high frequencies components of the impulse are naturally directed to ground by parasite capacitance or to other turns by stray capacitance between coils or turns.

As highlighted by R.J Beeckman and others, the consequence of this phenomena is that 80% of the voltage during short rise time (over 5 kV/µs) is concentrated on the first turns of the first coils. With SiC or GaN switch, that threshold is by far reached. [13, 14, 15].

Random wound motors are likely to have several exits turns in the vicinity of the first turns, thus increasing the electrical stress on turn-to-turn insulation system. This may result in the apparition of partial discharge in the first turns of a windings and lead to failure close to motor terminals. Indeed, most of the time, failures seem to be located either at very first or very last turns of one phase. [16]

Turn-to-turn electrical stress is thus at the same time function of the voltage level along the coils but also function of the rise time. A typical RLC (figure 4) model could be used to have qualitative conclusions about the effect of very fast impulse on stator coil depending on model parameter.

Figure 5 shows a typical simulated response of a coil submitted to a SiC turn-on switch with a DC bus of 270VDC at 6 different coils points. The harness length introduce a 3ns delay, almost no additional overvoltage. Parasitic capacitances of the converter are creating large voltage oscillations and represent a worst case scenario. Voltage propagation is non-uniform alongside the coil, creating very large voltage differences between turns of the same coil during the first instants after the switching. [17]

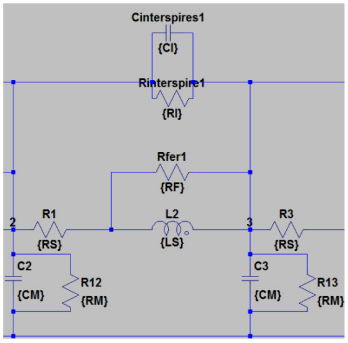

Figure 4. Typical RLC model 7 component cell used to simulate impulse voltage propagation along a coil (LTSpice)

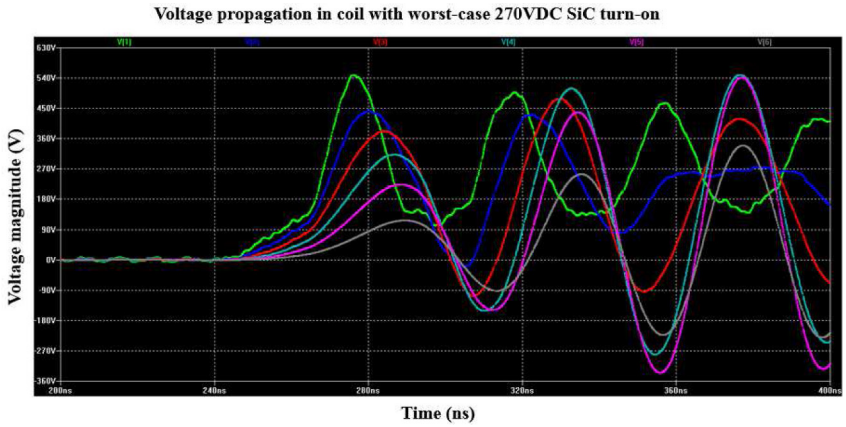

Figure 5. Example of voltage propagation of SiC turn-on switching along a motor coil (simulated with LTSpice)

Environmental Parameters

Besides electrical stress, we have seen previously than partial discharge inception voltage depends on pressure. Other parameters could play a role in weakening the insulation system quality like temperature and humidity. Some motors are pressurized or hermetically sealed or simply at cabin pressure such as fans. Other may be subjected to environment cycling, high temperature when in proximity of jet engines. Since temperature and humidity are very dependent of each other (through vapor pressure), this paper will only focus on the effect of altitude. The lowest test level has been set in accordance with partners at 100mbars, 52.000 feet, 16.000m altitude.

Electrical Motor Design

The following motor design is a standard insulated 540V MEA stator, rated at 10kW, to serve as a reference point and a representative sample to develop test procedures and equipment.

Classification of Electric Machine

Electric motors are a key element in the evolution towards more electric aircraft (MEA) and are classified as follows:

- Electrical generators, which convert mechanical energy into electrical energy;
- Electrical motors, which convert electrical energy into mechanical energy (usually rotating torque).

In this paper, we are particularly interested in AC electrical motors fed by PWM inverters. Indeed, these motors allow the development of any torque at any speed. Designing an electrical motor under aeronautical constraints is a very complicated process, as it requires to make a compromise between several aspects [18, 19], for example:

- Reliability;
- Power density;
- Thermal robustness;
- Control features and complexity;
- Complexity of design and fabrication;
- Cost.

Electrical motor with brushes requires high maintenance requirements. Additionally, it has a low torque density and it lacks of reliability. Therefore, candidate machines are limited to

- Permanent magnet synchronous motor ;
- Reluctance motor ;
- Induction motor.

The stator of these three types of electrical motors are relatively similar. It mainly consists in (figure 6):

- Winding: coils arranged spatially to create a rotating magnetic field.
- Magnetic circuit (core): a stack of ferromagnetic sheets glued together and insulated from each other.
- Electrical insulation system (EIS): prevents short-circuits in winding and allows the transfer heat (causes by the winding RI^2) between the copper and the core. Basic electrical insulation system is composed of
  - Turn-to-turn insulation
  - Phase-to-ground insulation;
  - Phase-to-phase insulation.

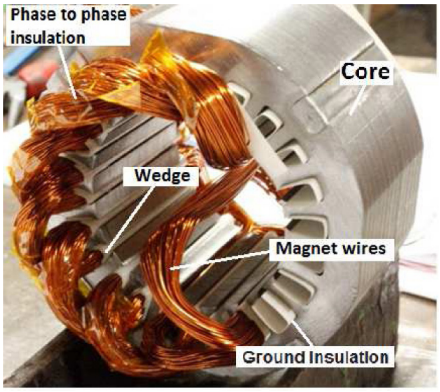

Figure 6. IRT stator with low voltage conventional insulation (during fabrication process)

Magnetic Circuit (Core)

In general, aircraft specifications limit either the axial length or the outside diameter of a motor, or sometimes both at the same time. At a defined axial length, the inner diameter of a stator represents the area traversed by the magnetic flux. This is a crucial parameter in the design process. Indeed, the electromagnetic torque is proportional to the square of this parameter [20]. There are two sources of magnetic flux in a permanent magnet synchronous motor:

- Permanent magnet ;
- Stator winding.

The width of the stator teeth and the yoke of the core (figure 7) is chosen at fair value allowing the magnetic circuit to transport the total magnetic flux without magnetic saturation phenomena. The material used in our case (silicone iron) allows 1.4T as a maximum induction. The choice of the number of slot depends on the following criteria [21]

- Winding factor
- Thermal exchange area
- Cogging torque
- Slots geometry

Stator Winding

This is a classical winding with: 3-phases, 8-poles, 1 slot per pole per phase and one phase by slot. (figure 10). The magnetic design and electrical design are strongly linked by the number of turns in series per phase (78 turns in our case).

Table 1. Stator winding characteristics

Number of phases	3
Number of slots	24
Number of poles	8
Coil pitch	1 - 4
Ø copper wire [mm]	0,5
Number of strands in //	2
Number of turns per coil	78
number of wires per slot	156
Number of way in //	4
Number of coil per slot	1
Coupling	Star

Characteristics must be chosen carefully to ensure that:

- The inductance of the motor remains in a well-defined interval.
- The back EMF of the motor at the maximum rotational speed is approximately equal to the supply voltage (this rule is valid for the motor operating without flux weakening technique).
- The current density (J) should be chosen according to the cooling solution. In our case, J=11A/mm^2 for a liquid cooling solution.

Chosen a 4 coils in parallel allows to adjust easily the number of turns in series per phase. The number of parallel strands (2 strands in our case) allows to choose a suitable diameter wire. A strand with a large diameter is difficult to manipulate during manufacturing process. In addition, it favors the appearance of the skin effect in high frequency applications. Using a strand with a very small diameter increases the insulation proportion in the slot at the expense of the copper proportion. Therefore, the current density increases and then the copper losses (RI^2). In addition to these two constraints, the wire diameter must be chosen to minimize the proportion of air in the slots volume.

One of our goals in the future works is to take into account the influence of the number of parallel strands on the partial discharge inception voltage (PDIV). Note that the structure of winding is a random-wound, usually used for voltages less than 1000 V and less than several hundred kW applications. To test each phase insulation separately, the neutral wire is not connected (figure 8, 9, 10)

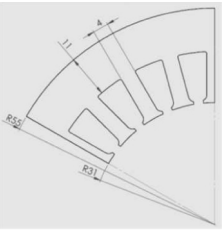

Figure 7. Main dimensions of the magnetic circuit (mm)

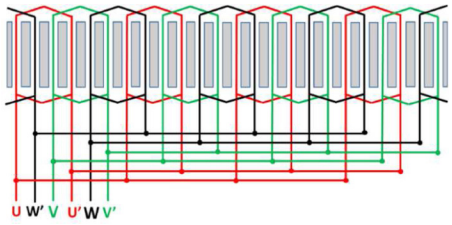

Figure 8. Overlapped winding diagram with neutral point not star connected

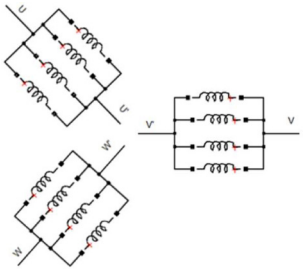

Figure 9. Equivalent circuit of stator design

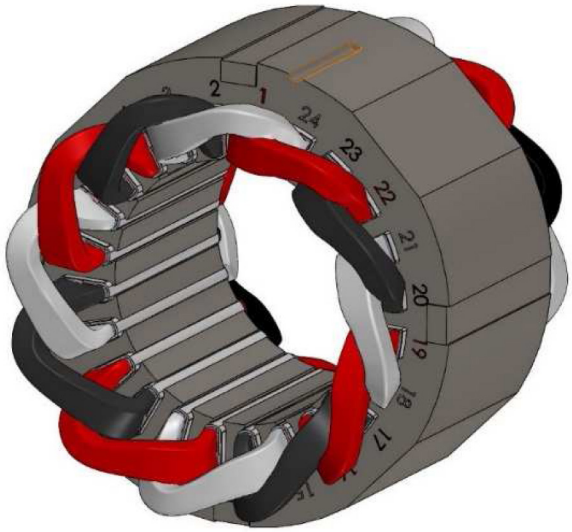

Figure 10. 3D modeling of stator and coils. End-winding connections are not represented.

It should be noted that a compromise has to be made between the representativity of the stator insulation system and the access to phase or coils. The decision has been made to only disconnect the neutral point and to left untouched phases start which are likely to be the most stressed area in the end-windings.

Electrical Insulation System (EIS)

Most of the random-wound windings are made with an enameled wire (Magnet wire). The enamel consists in polymer-based resin layers, it ensures the turn to turn insulation. In our case (1 coil per slot), the insulation between phases concerns only the winding heads. To avoid the risk of breakdown phenomenon, the axial length of the slot insulation (Phase-to-ground insulation) exceeds the length of the core by 3 mm on each side. The following tables summarize some characteristics of used insulation:

Table 2. Enamel wire properties (Norm IEC 60317-13)

Copper diameter [mm]		0,5 ±0,005
Grade		2
Class		H
Magnet wire diameter [mm]	Minimum	0,545
	Maximum	0,566
Voltage breakdown [V]		4600

Table 3. Insulation system reference and thickness

Insulation type		Reference	Thickness [mm]
Phase to ground	Slot cell	NOMEX 410- Class H	0,15
	Wedge	ISOVALFR4-Class H	0,5
Phase-to-phase		INTERTAPE-Class H	0,065
Coils connections and phase terminal		Siligaine – Class H	0,2

Development of Testing Procedures and Samples

To develop adequate test procedure for each insulation and relevant samples, one should first analyze the different case of electrical stress on each type of insulation.

Turn Insulation

Turn isolation is stressed by fast switching for adjacent turns in the coil. Only primary insulation (ie enamel of magnet wire) is tested.

Twisted Pair

Test on magnet wire alone are made with standard twisted pair. No modification are made to this well-known test set-up. Samples are thus realized according to usual standards and recommendations [22]. Twisted pair represents the worst-case scenario of the turn-to-turn insulation with one wire grounded while the other is at testing voltage. In coil, it means that the first turn is in the vicinity of the last turn in the slot or in the end-winding. 50 Hz AC voltage to test the insulation performance of the enamel wire will be used as recommended by standards.

Coils Impulse Test on Motor

The impulse test on coil is not meant to provide information on material but to assess how the final winding geometry is vulnerable to partial discharge create by fast switching . Winding process and operator preference when forming coils are obviously key factors in performance.

In random wound motor, it is very difficult to predict if one motor winding is sensitive to fast switching. Process repeatability will have to be ensured and will be critical in improving turn-to-turn performance all other things being equal. Design choice regarding number of wires per turn will also have to be taken into account, the higher the number, the most risk of worst-case scenario. (Figure 11). An impulse test on each coil separately (other coils and stator core are at floating potential) will be performed with fast rise time on the stator. (Figure 12)

Phase-to-Phase Insulation

Whereas turn-to-turn insulation is difficult to control in random wound motor and mainly depends on materials properties, number of wire per turn and coil forming process, phase-to-phase insulation in end-winding is supposed to be composed of both primary insulation (magnet wire) and phase-to-phase insulation (in our case, Kapton intertape with 65µm thickness) as shown in figure 13.

Winding Diagram Analysis

End-winding geometry is function of winding diagram (figure 8, 9, 10) already shown above. The parallel architecture with eight poles means that end-winding insulation between phases to be made with great care. Indeed, long connection between each of four coils will be needed and will result in a lot of overlap between respective phase connection wires. The use of glass-fiber reinforced silicone is typical of low voltage motor and is applied here. Specials recommendations were given to the coiler to have particular care when using silicone on coils connections and to use them as close as possible to slot as shown in figure 14.

Other winding diagram analysis may have led to different conclusions. For example, with four coils in series instead of parallels, only phase entrance and the first connection may have to be insulated with silicon.

Figure 12. Details of turn distribution during coils insertion

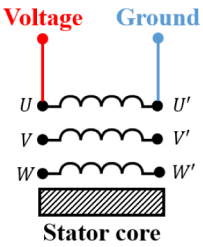

Figure 11. Schematic of coil impulse test

Figure 13. Details of phase to phase insulation during coil insertion

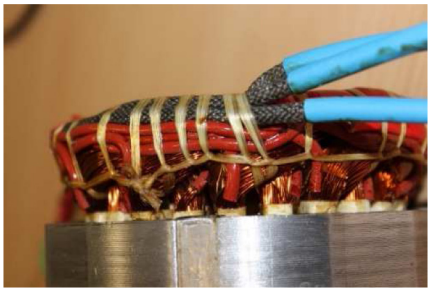

Figure 14. Details of phase terminal insulation and coils connections insulation. Siligaine appear in brown.

Inverter Drive Command Analysis

Before going into more details regarding the phase-to-phase test setup, it is important to recall how the machine is driven with typical PWM signal coming from an inverter drive (figure 15)

A three leg inverter has eight different configurations, listed in the following table and determined by its switch states.

Table 4. Correspondence between switches state and inverter drive configuration

Config.	K_1	K_2	K_3	K_4	K_5	K_6
0	0	1	0	1	0	1
1	1	0	0	1	0	1
2	0	1	1	0	0	1
3	1	0	1	0	0	1
4	0	1	0	1	1	0
5	1	0	0	1	1	0
6	0	1	1	0	1	0
7	1	0	1	0	1	0

Table 5. Correspondence between inverter drive leg state and inverter drive configuration.

i	0	1	2	3	4	5	6	7
λ_U	0	1	0	1	0	1	0	1
λ_V	0	0	1	1	0	0	1	1
λ_W	0	0	0	0	1	1	1	1

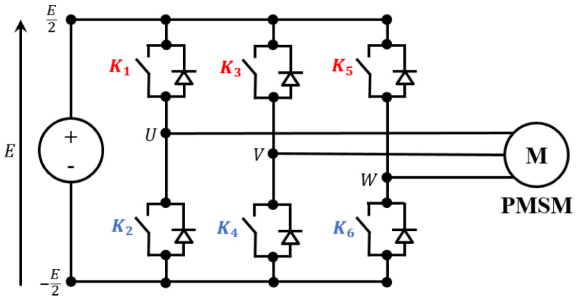

Figure 15. Schematic of inverter drive connected to permanent magnet synchronous motor.

By introducing leg state λ, calculation of phase-to-phase voltage and phase-neutral voltage will be easier. Table 5 lists leg state value function of inverter drive configuration

Under the assumption that the load is perfectly balanced (all phases are similar), it can be shown that voltage between each phase and the neutral point for star connected motor is function of inverter drive configuration with the following relationship.

$$\begin{bmatrix} V_{UN}(k) \\ V_{VN}(k) \\ V_{WN}(k) \end{bmatrix} = \frac{E}{3} \cdot \begin{bmatrix} 2 & -1 & -1 \\ -1 & 2 & -1 \\ -1 & -1 & 2 \end{bmatrix} \cdot \begin{bmatrix} \boldsymbol{\lambda_U(k)} \\ \boldsymbol{\lambda_V(k)} \\ \boldsymbol{\lambda_W(k)} \end{bmatrix} \quad (17)$$

It can also be shown that voltage between phases for the same star connected motor is function of inverter drive configuration according to the following relationship.

$$\begin{bmatrix} V_{UV}(k) \\ V_{VW}(k) \\ V_{WU}(k) \end{bmatrix} = \mathrm{E} \cdot \begin{bmatrix} 1 & -1 & 0 \\ 0 & 1 & -1 \\ -1 & 0 & 1 \end{bmatrix} \cdot \begin{bmatrix} \boldsymbol{\lambda_U(k)} \\ \boldsymbol{\lambda_V(k)} \\ \boldsymbol{\lambda_W(k)} \end{bmatrix} \quad (18)$$

It should be noted that, for both phase to phase and phase-neutral voltages, two configurations (configuration n°0 and n°7) are not needed to be taken into account anymore for partial discharge analysis between phases. Indeed, no voltage difference between phases exists in such configurations. In steady state, after switching propagation, the phase-to-phase voltage is linearly distributed along turns of the three phases. On the remaining configuration, the higher electrical stresses locations that may trigger partial discharge between phases can be demonstrated from phase to phase voltage analysis listed in table 6.

Table 6. Phase to phase voltage (at terminals) function of inverter drive configuration.

Configuration	V_{UV}	V_{VW}	V_{WU}
1	**E**	0	**-E**
2	**-E**	**E**	0
3	0	**E**	**-E**
4	0	**-E**	**E**
5	**E**	**-E**	0
6	**-E**	0	**E**

A more convenient way to present the partial risk between phases is presented in table 7.

Table 7. Phase insulation at risk function of inverter drive configuration.

Phase to phase insulation	Configuration
UV	1,2,5,6
VW	2,3,4,5
WU	1,3,4,6

From the above discussion and analysis, two different phase to phase tests are need to fully characterize the partial discharge insulation performance.

Worst-Case Bipolar and AC Phase to Phase Test

With the neutral point disconnected, it is easy to test one phase at a time with others being grounded with AC 50Hz voltage. But, one should keep in mind that this electrical stress is not representative of the star-connected case where the neutral point voltage is oscillating between 2/3 and 1/3 of DC bus. This test is more severe than operating conditions for the phase to phase insulation but is simple to carry out. A 1kHz bipolar square test will also been carried out to check the difference with AC. (figure 16)

Representative Impulse to Phase to Phase Test

In order to test phase-to-phase insulation in more representative way, the neutral points have to be star-connected and impulse with a fast rise time should be performed. By rotating test configuration according to inverter drive configuration, electrical stress will be correctly distributed alongside coils and conclusions could be drawn regarding operational performance.(figure 17)

Twisted Pair

A twisted pair could also represents the phase to phase insulation in the winding if phase-to-phase insulation is not applied properly. If the motor phase-to-phase result are very similar to the twisted pair test, it means that phase-to-phase insulation is not properly made in the end-winding.

Phase-to-Phase Motorette

The motorette is also a usual test sample in partial discharge testing. Here, a modification has been made to represent phase to phase insulation system only. Two short specific coils (50 turns) have been made and are isolated by the phase-to-phase insulation (intertape). This sample is made to represent end-winding stress, the two short coils are thus pressed against each other. (figure 18). This test allows preliminary characterization of the combination of magnet wire and phase-to-phase insulation. The test will be performed at AC 50Hz voltage and 1kHz bipolar square voltage

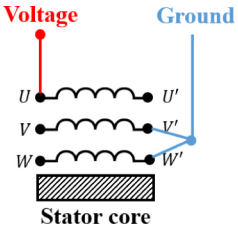

Figure 16. Worst case AC phase-to-phase test.

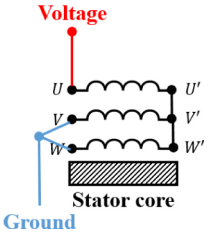

Figure 17. Representative impulse phase-to-phase test

Figure 18. Detail of phase-to-phase motorette test set-up

Figure 19. Detail of phase-to-ground insulation.

Phase-to-Ground Insulation

The phase-to-ground stress depends on how the stator core is connected to the electrical network in an MEA (figure 19). There is actually a big difference of electrical stress between a 0-540VDC network with stator core connected to low voltage and a ± 270VDC network with the stator core connected to the mid-point. The former is supposed to be unipolar with a 540V maximum peak amplitude while the latter is bipolar with 270V maximum peak amplitude. Apart from this nuance, the phase-to-ground test is pretty straightforward and can even be carried out with the neutral point connected, testing all phases at the same time. Both AC and 1kHz bipolar square voltage waveform will be tested.

Phase-to-Ground AC and Bipolar

One phase at a time will be connected to the power supply, the stator core is grounded as shown in figure 20.A voltage waveform of 1khz (50% duty cycle) bipolar square will also be tested.

Phase-to-Ground Motorette

In order to test the combination of slot paper and magnet wire, piece of sheet metals are folded to represent a slot with similar dimension compared to the stator. Insulation paper is placed with the same care as in the stator with an excess length of 3mm. A coil of 50 turns is then slotted and push against the paper thanks to foam. This test will be performed with AC 50Hz voltage applied to the coils and metal sheets grounded. (figure 21)

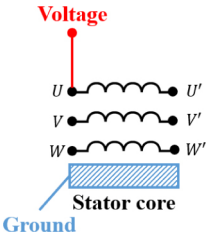

Figure 20. Phase-to-ground test.

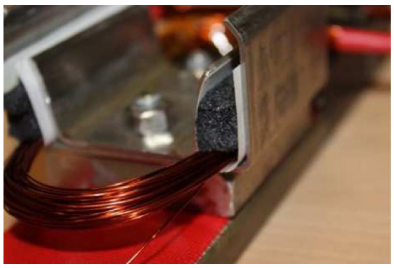

Figure 21. Detail of motorette phase-to-ground set-up

Experimental Set-Up

Power Supplies

High Speed High Voltage Power Amplifier

Associated with a Tektronix AFG3022 dual channels arbitrary waveform generator, the Trek 10/40A-HS amplifier is able to deliver 10kV peak and a maximum of 40mA RMS current with a bandwidth of 23 kHz. This versatility allows different voltage waveforms to be tested such as AC at various frequency, square bipolar with adaptable duty cycle, frequency and other point-per-point signals.

High Voltage Bipolar Inverter

The PWM like voltage shape is created by a homemade PWM inverter associated with a high voltage power source up to 1.7 kV DC (and back up current peak up to 50 A). This bipolar pulse like generator allows testing of low voltage electric motors coils. The IGBTs components used are able to withstand around 1.5 kV, almost full use of the high power supply, to try to PDIV. The bipolar inverter drive part is completely adaptable such duration of the pulses, the time between pulses, the switching frequency and duty cycle.

High Voltage Measurements

Voltage level are monitored using a Testec TT-SI 9010A (1/1000 ratio) active differential probe whose bandwidth is 70MHz.

Signal Acquisition

Analog to Digital Conversion

Data are displayed and recorded using a either a Tektronix MSO 5204 Digital Oscilloscope with a 2 GHz numerical bandwidth and 5 GS/s sampling rate for each channel or Keysight DSOS204A oscilloscope with a sampling rate of 20GSa/s and numerical bandwidth of 2GHz. All measurements were made in peak detect mode with sampling frequency fixed at 5GS/s for both instruments.

Analog High Pass-Filtering

When performing measurement using non-intrusive sensor, it is usual to connect high-pass analog filter to remove noise coming from inverter drive switches or power amplifier. Typical cut-off frequency range from 25MHz to 200MHz.

Partial Discharge Sensors

Technological research at IRT Saint-Exupéry are focused on non-intrusive sensors. These sensors and associated method have already prove to be effective for detecting partial discharge on-line on both electric motor in automotive [24] and aeronautic test benches [3].

Capacitive Sensor

The first non-intrusive sensor used to detect partial discharge is taking advantage of the capacitive effect. In other words, partial discharge small current impulses are transduced into voltage variations through the capacitance between the copper wire and oscilloscope impedance. In order to increase signal amplitude, the capacitive effect could be enlarged using metallic adhesive, expanding capacitive surface, directly on the power cable and making in effect a cylindrical electrode. Then, the jack-SMA sensor is put in contact with the metallic adhesive to gather analog variations of partial discharge signals.

Inductive Sensor

The second non-intrusive sensors is a wideband fast current transformer (FCT) Bergoz FCT-016-1.25. The magnetic core is made of cobalt-based amorphous and nanocrystalline alloys which provide high permeability and very fast rise time. Low cut-off frequency (-3dB) is 9.5kGz and upper cut-off frequency (-3dB) is 1.75GHz. Since this FCT is better known than the capacitive sensor on the basis of previous experiments, the former will be used as a reference.

Environmental Conditions

All the tests have been carried out within a grounded vacuum chamber, acting as a faraday chamber, connected to a vacuum pump. The system is currently able to pressure from atmospheric to 20mbars with an accuracy of +/- 5 mbars.

Non-Intrusive Partial Discharge Detection

In the context of the detection of partial discharges in equipment supplied by PWM like voltage, a key challenge is to distinguish the partial discharge signal with respect to electromagnetic noise induced by the fast switching converters. Usually, the magnitude of the signal associated to partial discharges has amplitude of several tens of mV while the amplitude of the noise signal is of the order of several hundred mV and depends on the amplitude of the voltage and its rise time (dynamic of voltage increase). From a frequency point of view, the spectrum of a discharge may extend to the GHz while the noise spectrum does not extend beyond a few hundred of MHz.

Noise Source

External interferences (usually of very high amplitude comparable to PD signal) directly affect the sensitivity and reliability of the acquired PD data. Thus, to be recognized as DP, the detected signal should appear with sufficient recurrence and be large enough to be

considered as something other than just random noise.The main sources of noise are divided in four categories classified by the type of interferences produced [25]:

- The periodic pulse interferences caused by power or other periodical operation of electronics,
- The spectral interference from eg broadcast radio AM, FM or communication systems,
- The stochastic pulse interference, caused by occasional events related to power electronics, lightning strokes…
- Other noise involving interference of the measurement circuit and ambient noise

In most cases, these external interferences can cause false indications, thereby reducing the credibility of the PD measurements as a diagnostic tool. Ever since this problem was recognized, extensive research work has been pursued in this area and several techniques for suppressing these external interferences have been proposed. Narrow band detectors achieved some success; better results were obtained by balanced bridge arrangements and by pulse discrimination circuits. But, such analog noise suppression methods are cumbersome, require additional equipment, and need critical adjustments, which might not be very easy, under on-site conditions. Fig. 22 shows that it is impossible to distinguish the presence of discharge. The noise amplitude induced by the switching is too large compared to the possible PD magnitude.

Noise Suppression Techniques

With the advent of high-speed computers and fast A/D converters, digital PD measurements became a reality, and soon after many digital methods for noise suppression evolved, These methods have yielded varying degrees of success. We mentioned below some of these methods of noise suppression based on several parameters.

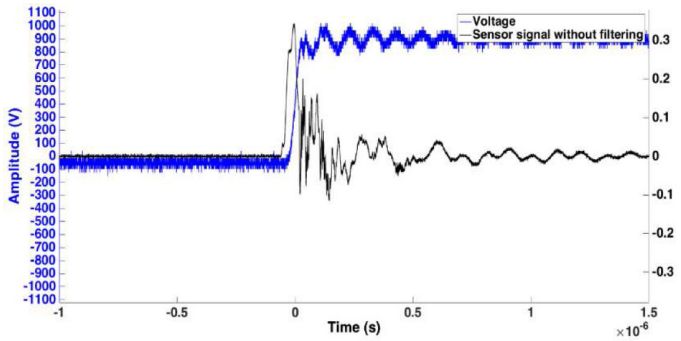

Figure 22. Noisy signal induced by switching (black)

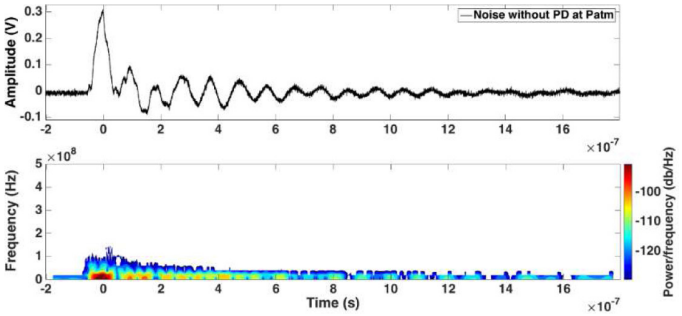

Figure 23. Noisy signal induced by switching without PD (top curve) STFT of noise without PD (lower curve)

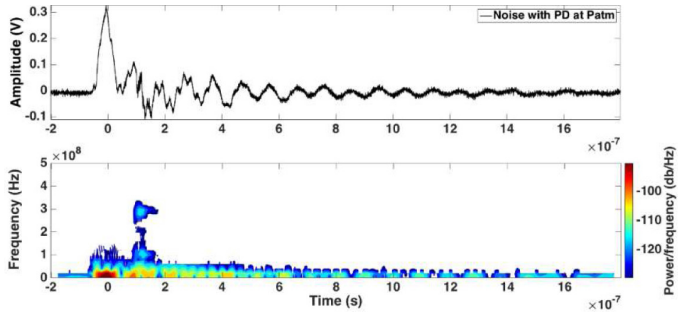

Figure 24. Noisy signal induced by switching with PD (top curve) STFT of noise with PD (lower curve

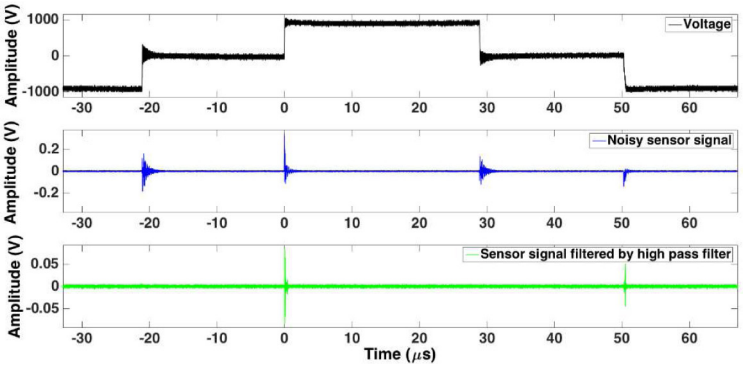

Figure 25. Voltage (black) Noise induced by switchings (blue) PDs signal after filtering by 150 MHz high-pass filter (green) during coil impulse test.

All these methods were compared according to the mean squared error (MSE) between the raw signal and the noise-suppressed signal as well as the execution time of filtering in [26]. By definition, the normalized MSE is:

$$MSE = \frac{\sum_{i=0}^{n}[Y(i) - X(i)]^2}{n\sigma_n^2} \quad (19)$$

X is is the noisy sequence, Y the filtered sequence, n the number of samples for which X is defined and σ_n^2 the total noise power. Based on these criteria, methods of Wavelet Denoising and High-pass Filtering are most effective. It is therefore necessary to remove this noise prior to intend to detect any PDs. The easiest solution is to filter the signal with a high-pass filter. Nevertheless, using a filter often results in a loss of signal information regarding the content of frequency components below the cut-off frequency.

In order to analyze the frequency spectrum of the discharge for systems fed by inverter, two kinds of measurements are performed, Acquisitions of the noise existing for voltage lower than the PDIV (≈ PDIV - 10 V) and higher than the PDIV were performed. Note that in that case, the PDIV value was determined using a high-pass filtering. The Short-Time Fourier transform (STFT) results reported in Fig. 23 shows that the spectral energy of the disturbance spreads up to 150 MHz, but only during the switchings "on/off" of the voltage. Thereafter, the remaining ringings, are negligible above 100 MHz. Under PDs, in Fig. 24, we can see that the spectral energy spreads up to 350 MHz. It is therefore possible to filter the noise while recovering part of the signal of the PD. However, the research of this cutoff frequency may be complex and will depend of the user experience. It is therefore necessary to use an automated method that allows matching to all configurations. Thanks to the observations obtained using the STFT, the cut-off frequency is set to 150 MHz (fig 25)

Tests Results

All tests were performed around ten times each to ensure PDIV and PDEV repeatability, results presented are thus average of several measurements. All standard deviations range from 5 and 10%. Coil impulse test at low pressure data are not presented due to the lack of accuracy in the detection method.

Turn Insulation Results

Table 8. Twisted pair results with AC 50Hz on twisted pair sample.

kV peak - AC 50Hz – twisted pair			
Atmospheric pressure		100 mbars pressure	
0,75	0,71	0,42	0,38

Table 9. Coil impulse with 5kV/µs at 10Hz

kV peak – impulse test - stator			
Coil	Atmospheric pressure		100 mbars pressure
Coil U	0,78	0,71	Not enough accuracy to guarantee results quality
Coil V	0,78	0,63	
Coil W	0,81	0,73	

Phase to Phase Insulation Results

Table 10. Worst case AC phase to phase test

kV peak – AC 50 Hz - stator				
Coil	Atmospheric pressure		100 mbars pressure	
U / VW	1,27	1,20	0,62	0,54
V / WU	1,16	1,10	0,62	0,57
W / UV	1,15	1,10	0,68	0,65

Table 11. Worst case bipolar phase to phase test

kV peak – Bipolar 1kHz – 50% DC - stator				
Coil	Atmospheric pressure		100 mbars pressure	
U / VW	1,17	1,10	0,54	0,50
V / WU	1,04	0,97	0,56	0,53
W / UV	1,05	1,00	0,59	0,53

Table 12. Representative impulse phase to phase test with 5kV/µs at 10Hz

kV peak – impulse test on motor coils – star connected			
Coil	Atmospheric pressure		100 mbars pressure
U / VW	1,26	1,07	Not enough accuracy to guarantee results quality
V / WU	1,38	1,22	
W / UV	1,34	1,20	

Table 13. AC phase to phase test

kV peak –- AC 50Hz – motorette			
Atmospheric pressure		100 mbars pressure	
1,24	1,12	0,55	0,49

Phase to Ground Insulation Results

Table 14. AC phase to ground

kV peak– AC 50 Hz - stator				
Coil	Atmospheric pressure		100 mbars pressure	
Coil U	1,54	1,44	0,64	0,61
Coil V	1,46	1,42	0,64	0,58
Coil W	1,51	1,46	0,66	0,62

Table 15. Bipolar phase to ground

kV peak – Bipolar 1kHz – 50% DC - stator				
Coil	Atmospheric pressure		100 mbars pressure	
Coil U	1,43	1,40	0,66	0,63
Coil V	1,32	1,26	0,66	0,63
Coil W	1,44	1,40	0,63	0,60

Table 16. AC phase to ground

kV peak –- AC 50Hz – motorette			
Atmospheric pressure		100 mbars pressure	
1,58	1,44	0,65	0,54

Discussion

General Remarks

Testing Conditions Discrepancies

Impulse testing (table 9 and 12) and twisted pair (table 8) tests were made at Laplace laboratory whereas all others were made at IRT Saint-Exupéry on different days. Some discrepancies (especially regarding phase-to-phase tests result) could be down to a different level of background noise in the laboratory as well as different atmospheric conditions regarding pressure, temperature and humidity.

Non-Intrusive Detection Performance with Impulse Testing at Low Pressure

Impulse testing detection at reduced pressure proved to be difficult. Indeed, it is know that frequency contents of partial discharge is changing with pressure. [4] As our detection with impulse relies on filtering, it was difficult to be sure within a 5-10% standard deviation target of PDIV and PDEV, so data were discarded and not reported here.

Difference between Bipolar 1 kHz and AC 50Hz

An approximately 100V peak difference is found between same insulation test with a different waveforms, namely AC 50Hz and 1kHZ bipolar (table 10 and 14, table 11 and 15 respectively). Several causes could explain this difference.

First, PD detection accuracy at oscilloscope with a 100ms window observation (5 periods of AC 50Hz) could be different than a 5ms windows (5 periods of bipolar 1 kHz) regarding background noise level with an advantage for the latter.

Another explanation may be the difference of signal period that may have a cumulative effect on PDIV or the fact that a bipolar pulse of 500µs has a quicker rise time than 50Hz sine. It is known from IEEE standard that the rate of voltage increase and previous history of insulation could have an impact of PDIV level.

Impact of Pressure

As expected, a 100mbars pressure is largely decreasing PDIV compared to atmospheric pressure. It would be useful to have a single proportional factor to estimate low pressure PDIV from atmospheric pressure PDIV. It does not seem from results that such a simple transformation exists globally for the stator. It may be true though for each insulation taken in isolation, especially twisted pair sample.

General Level of PDIV

From a quantitative point of view, it could be said that this stator would have withstood a typical 540VDC converter at day one for phase-to-phase and phase-to ground insulation with most PDIV above the 1,1 kV level which is twice the DC bus and for worst case testing procedure.

A doubt could be raised for impulse testing result since 800V peak voltage could be reached with a combination of harness length and high dV/dt. The obvious solution would be to choose a grade 3 magnet wire to increase turn-to-turn PDIV.

These general considerations being said, one should keep in mind that no varnish nor impregnation have been made on this stator. The varnish, if correctly applied, is supposed to enhance insulation system properties aside its mechanical and thermal properties.

Turn Insulation Results Analysis

Twisted pair results are fairly consistent with what could be expected from a usual 0.5mm grade 2 magnet wire at atmospheric pressure.

It can be seen that the twisted pair results are only a little above impulse test for the 3 coils. That means that the worst case scenario seems to be avoided with this coil forming technique even if the 30V peak of difference could be down to measurement accuracy. No absolute conclusions can thus be drawn, but insulation performance regarding this turn stress are relatively consistent for each phase which suggest that the winding are fairly similar between each other

Phase to Phase Insulation Analysis

Compared to twisted pair result, PDIV of all phase to phase test suggest that the Kapton isotape is indeed efficiently used and left no magnet wire of different phase in close proximity. Depending on the voltage waveform, a 300 to 400V peak difference is observed with turn-to-turn results. Appendix A is showing typical picture of phase to phase discharge

As expected, the impulse test with star connected phase displays larger PDIV (around 100V peak more) than worst case AC and bipolar testing. From voltage distribution analysis when the stator is star connected, a higher difference may have been expected. That would be consistent with the low results of impulse testing found in turn insulation results.

Two assumptions could explain this relatively close PDIV between worst case AC and impulse. First, the speed of the switching is of critical importance and a slower rise may have led to a higher difference. Or, the partial discharge is located in the end winding between beginning and end of each coil and the neutral point connection is not that much of a difference regarding the electrical stress. A combination of the two explanation is also plausible.

Motorette result are, on average, fairly consistent with similar waveform test (AC 50 Hz) at atmospheric pressure which suggest that the motorette representation of phase insulation is in agreement with the stator. A larger difference is although found in low pressure test which may be explained by a difference in geometry as the two coils are just taken in close vicinity without a whole end-winding. That may suggest that low pressure discharge in phase-to-phase isolation may be limited by the proximity of other coils.

Phase to Ground Insulation Analysis

On average, phase-to-ground PDIV levels are fairly consistent across all sample at low and atmospheric pressure which suggest that slot modeling of the motorette is appropriate although it seems to produce better results. Coils position related to slot may be the cause since fill factor are not comparable with stator. Appendix B is showing typical low pressure slot discharge.

Summary and Conclusions

This paper illustrates the reason behind advanced partial discharge testing for MEA motors, especially the voltage increase of MEA network. The paper provides detailed review of the electrical stress creation in e MEA electromechanical chains. More precisely how harness length and fast switching are actually stressing the insulation system. Simple models have been provided to illustrate the qualitative effects of those drastic changes. In order to define and apply testing procedures, a typical MEA stator have been designed and relevant details regarding the insulation systems are provided.

This study showed that insulation performance of a MEA stator before varnishing could be estimated using appropriate test procedure and samples. The data offers evidence of the notable influence of pressure on PDIV levels. The data illustrates the fact that proposed procedures and samples seems appropriate to assess insulation performance.

Details of testing procedure was provided according in comparison with operational electrical stress. The ability of non-intrusive sensor associated with numerical signals processing was also demonstrated although improvements have to be made regarding low pressure impulse testing.

We recommend that motor designers carry out numerous testing before choosing an insulation system. Since the weakest insulation performance is related to turn-to-turn stress, it is highly recommended to perform impulse testing on each phase (star-connected or not).

Future Work and Improvements

As a conclusion of this technical report, numerous points have to be further investigated to improve partial discharge testing on MEA motor with non-intrusive sensor.

- Robustness of non-intrusive detection at low pressure with impulse voltage
- Representativity of motorette test to be reinforced, especially regarding slot fill factor and proximity effect in phase-to-phase.
- Characterization of noise level prior detection as a sensitivity calibration with non-intrusive sensor
- Measurement of relevant environmental quantities when measurements are performed
- Impact of voltage waveform, period and rise time on PDIV level, especially the difference between AC and bipolar
- Study of the effect of varnishing and end-winding compression
- Study of the of temperature and humidity

References

1. Cotton, A. Nelms and Husband M., "Higher voltage aircraft power systems," in IEEE Aerospace and Electronic Systems Magazine, vol. 23, no. 2, pp. 25-32, Feb. 2008. doi:10.1109/MAES.2008.4460728
2. Lebey T., Cella B., Billard T. and Abadie C., "Partial discharges in aeronautics: the last frontier?" Properties and Applications of Dielectric Materials (ICPADM), 2015 IEEE 11th International Conference on the, Sydney, NSW, 2015, pp. 268-271. doi:10.1109/ICPADM.2015.7295260
3. Cella B., Lebey T. and Abadie C., "Partial discharges measurements at the constituents' level of aerospace power electronics converters" Electrical Insulation Conference (EIC), 2015 IEEE, Seattle, WA, 2015, pp. 274-277. doi:10.1109/ICACACT.2014.7223587
4. Grosjean D. F., Schweickart D. L., Kasten D. G., Sebo S. A. and Liu X., "Development of procedures for partial discharge measurements at low pressures in air, argon and helium," in IEEE Transactions on Dielectrics and Electrical Insulation, vol. 15, no. 6, pp. 1535-1543, December 2008. doi:10.1109/TDEI.2008.4712655
5. IEEE Guide for the Measurement of Partial Discharges in AC Electric Machinery - 2010
6. Bartnikas R. and McMahon E. J., “Engineering dielectrics - Volume 1 - Corona measurements and interpretation”, American Society for Testing and Materials - STP669, published in 1979
7. Roboam X., "New trends and challenges of electrical networks embedded in “more electrical aircraft”," Industrial Electronics (ISIE), 2011 IEEE International Symposium on, Gdansk, 2011, pp. 26-31. doi: 10.1109/ISIE.2011.5984130
8. Rosero J. A., Ortega J. A., Aldabas E. and Romeral L., "Moving towards a more electric aircraft," in IEEE Aerospace and Electronic Systems Magazine, vol. 22, no. 3, pp. 3-9, March 2007. doi: 10.1109/MAES.2007.340500
9. Karimi K.J., “Future Aircraft Power Systems - Integration Challenges”.2007
10. Moir I., Seabridge A. “Aircraft Systems: Mechanical, Electrical and Avionics Subsystems Integration, 3rd Edition”, August 2011
11. Persson E., “Transients Effects in Application of PWM Inverters to Induction Motors”, IEEE Transactions on Industry Applications, vol.28, no.5, Sep./Oct.1992, pp. 1095-1101 doi: 10.1109/28.158834
12. Rotating Electrical Machines - Part 18-41: Qualification and Type Tests for Type I - Electrical Insulation Systems Used in Rotating Electrical Machines Fed from Voltage Converters, IEC 60034-18-41 - TS Ed. 1.0, 2007
13. Beeckman R.J., “Inverter drive issues and magnet wire responses", Proceedings of Electrical Insulation Conference and Electrical Manufacturing and Coil Winding Conference, IEEE, 1999, pp.139-141. doi: 10.1109/EEIC.1999.826195
14. Bonnett A.H., “Analysis of the impact of pulse-width modulated inverter voltage waveforms on AC induction motors", IEEE Transactions on Industry Applications, Vol. 32, No. 2, March-April 1996, pp. 386-392. doi: 10.1109/28.491488
15. Stone, G.C., Campbell, S.R., Lloyd, B.A., Tetreault, S., “Which Inverter-Fed Drives Need Upgraded Stator Windings”, IAS/PCA, Salt Lake City, May 7-12/2000. doi: 10.1109/PCICON.2000.882771
16. Melfi M., Sung J., Bell S. and Skibinski G., "Effect of surge voltage risetime on the insulation of low voltage machines fed by PWM converters," Industry Applications Conference, 1997.

Thirty-Second IAS Annual Meeting, IAS '97., Conference Record of the 1997 IEEE, New Orleans, LA, 1997, pp. 239-246 vol.1. doi: 10.1109/IAS.1997.643034

17. Duchesne S., Mihaila V., Velu G. and Roger D., "Study of wire distribution in a slot of a motor fed by steep fronted pulses for lifetime extension," Electrical Insulation (ISEI), Conference Record of the 2012 IEEE International Symposium on, San Juan, PR, 2012, pp. 601-605. doi:10.1109/ELINSL.2012.6251541
18. Krishnan R. and Bharadwaj A. S., "A comparative study of various motor drive systems for aircraft applications," Industry Applications Society Annual Meeting, 1991., Conference Record of the 1991 IEEE, Dearborn, MI, USA, 1991, pp. 252-258 vol.1. doi: 10.1109/IAS.1991.178163
19. Cao W., Mecrow B. C., Atkinson G. J., Bennett J. W. and Atkinson D. J., "Overview of Electric Motor Technologies Used for More Electric Aircraft (MEA)," in IEEE Transactions on Industrial Electronics, vol. 59, no. 9, pp. 3523-3531, Sept. 2012. doi: 10.1109/TIE.2011.2165453
20. Fodorean D., Miraoui A., “Dimensionnement rapide des machines synchrones à aimants permanents (MSAP) “, technique de l’ingénieur, D3554, 2009.
21. Dogan H., Wurtz F., Foggia A., Garbuio L. “Analysis of Slot-Pole Combination of Fractional-Slots PMSM for Embedded Applications“, 2011. doi: 10.1109/ACEMP.2011.6490669
22. Boucenna N., ”Contribution à la modélisation en compatibilité électromagnétique des machine électriques triphasées”. Ph. D: Electrical engineering.CACHAN: SATIE-ENS Laboratory, 2014.
23. “IEC 60851:2008 Winding wires - Test methods.” 2008.
24. Billard T., Lebey T., Fresnet F., “Partial discharge in electric motor fed by a PWM inverter: off-line and on-line detection," in Dielectrics and Electrical Insulation, IEEE Transactions on , vol.21, no.3, pp.1235-1242, June 2014. doi:10.1109/TDEI.2014.6832270
25. Satish L. and Nazneen B., “Wavelet-based denoising of partial discharge signals buried in excessive noise and interference,” IEEE Trans. Dielectr. Electr. Insul., vol. 10, no. 2, pp. 354-367, Apr. 2003. doi: 10.1109/TDEI.2003.1194122
26. Sriram S., Nitin S., Prabhu K. M. M., and Bastiaans M. J., “Signal denoising techniques for partial discharge measurements,” IEEE Trans. Dielectr. Electr. Insul., vol. 12, no. 6, pp. 1182-1191, Dec. 2005. doi: 10.1109/TDEI.2005.1561798

Contact Information

Please direct contact to Dr. Thibaut Billard, research engineer and electromechanical designer at IRT Saint-Exupéry on temporary assignment from Liebherr Aerospace, Toulouse, France
Thibaut.billard@irt-saintexupery.com

Acknowledgements

The information presented in this paper is the result of contributions from many team members of the more electrical aircraft - reliability and integration project. The authors would like to thank the following individuals for thoughtful discussions and input: Nicolas Chadourne, Dr. Bernardo Cougo and Dr. Thierry Lebey.

Definitions/abbreviations

AC - Alternative Current

APU - Auxiliary Power Unit

ATU - Auto Transformer Unit

DC - Direct Current

EBHA - Electric backup hydraulic actuator

ECS - Environment Control System

EDP - Electrically Driven Pump

EHA - Electro Hydrostatic Actuator

EIS - Electrical Insulation System

EMA - Electromechanical Actuator

EMF - Counter-electromotive force

FCT - Fast Current Transformer

FFT - Fast Fourier Transform

GaN - Gallium Nitride

IDG - Integrated Drive Generator

IRT - Institute of Technological Research

MEA - More Electrical Aircraft

MW - Magnet Wire

PD - Partial discharge

PDEV - Partial Discharge Extinction voltage

PDIV - Partial Discharge Inception voltage

PWM - Pulse Width Modulation

SiC - Silicon Carbide

STFT - Short Time Fourier Transform

UAV - Unmanned Air Vehicle

VFG - Variable Frequency Generator

APPENDIX

Appendix A

Appendix B